3. RESULTS

3.1 Intracellular recording of DSGCs

Direction selective ganglion cells (DSGCs) in the isolated intact rabbit retina were visualized under a fluorescence microscope. Cell bodies were pre-labeled with DAPI by intraocular injection. We looked for DSGCs on the basis of their crescent-shape somata on the ganglion cell layer (Fig. 3C, 3D). A cell was selected and impaled with a sharp microelectrode under visual control. Usually the cell fired randomly at the initial stage after successful penetration, but the resting membrane potential became stable in a few minutes. The DSGCs were known that they fired action potentials to the onset of both light and dark illumination in the gray background. Therefore, when the resting membrane potential restored, a flash light square size was first projected to the retina to confirm the ON-OFF response and to localize its receptive field center. We then switched the stimulus to a moving object in order to determine the prefer-null axis of the DSGC. A light bar moved in 12 directions was projected to the retina again, and the recording was made (Fig. 5). Two apparent physiological properties of DSGCs were observed. First, when the leading edge of the moving light bar entered the receptive field, a DSGC generates ON responses. In contrast, a DSGC evoked OFF responses when the trailing edge went through the receptive field (Fig. 6, 7). Second, the cell exhibited plenty spikes when the stimulus moved in the preferred direction, but fired weakly in the opposite direction (Fig. 5, 6, 7, 8A-8D). Notably, DSGCs hyperpolarized before the stimulus

arrived (Fig. 7). The phenomenon suggests that there is a spatially offset inhibition in the mechanism of direction selectivity, and this is consistent with the result of patch-clamp recording (Fried et al., 2005).

By converting the recorded spike responses into polar plots, the DSGCs exhibit highly selectivity for the direction, and the measured preferred directions were usually fallen on one of the four cardinal directions (Fig. 8A-8D). However, spike response of the orientation selective ganglion cells (OSGCs), and other non-DSGCs have entirely different patterns (Fig. 8E, 8F). The *DI* values of these cell types also revealed obvious difference: *DI* of DSGCs was 0.78 ± 0.16 (mean ± s.d., n=15), *DI* of OSGCs was 0.14 ± 0.08, and *DI* of other non-DSGCs was 0.12 ± 0.06 (Fig. 9).

3.2 Morphology of direction selective ganglion cells

The recorded DSGCs were filled with fluorescent tracers to visualize the full contents and fine structures of their dendritic morphology. The DSGCs recorded in this paper were ranged from the central retina (except visual streak) to mid-periphery. Most of them possess similar morphology. The most distinctive character of the DSGC is bi-stratification (Fig. 10). In addition, their dendrites branch regularly and curve back to form a complicated lattice-like appearance, regardless of the stratification (Amthor et al.,1989b; Yang and Masland, 1994) (Fig. 11A, 11B, all DSGCs in this study were represented in green for consistency unless otherwise stated). However, we found that dendrites on the ON sub-lamina are often remarkably less and sparser than the OFF dendrites (Fig.

11C-11F). The primary dendrites are thick, but the diameters of dendrites become less with the process extending. Since no other ganglion cells with these characters have been reported in the rabbit retina, we can unambiguously identify DSGCs even without performing physiology experiments (Rockhill et al, 2002).

In the central retina, the dendritic fields of DSGCs are small (200-300 μm) and sometimes tend to be asymmetric (Fig. 12A, 12B). The dendritic arbors become larger and more symmetric with increasing eccentricity. This results that the diameters of DSGCs' dendritic fields could be over 700 μm in the periphery (Fig. 12C, 12D). No obvious relationship was found between the physiology information and the dendritic branching pattern (Yang and Masland, 1994).

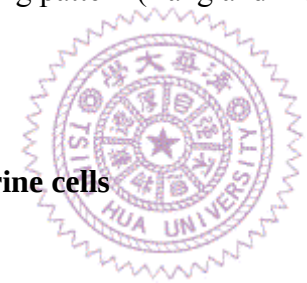

3.3 Morphology of starburst amacrine cells

Starburst amacrine cells were identified effortlessly by their DAPI-labeled bright round somata in the ganglion cell layer (Fig. 3C, 3D). Likewise, fluorescent tracers were injected to visualize their morphology. The morphology of SACs also has conspicuous characters. Their dendrites extend outward radially from any direction, and exhibit a soma-centered starburst firework appearance (Fig. 13, all SACs in this study were represented in red for consistency unless otherwise stated). According to the distance from soma, the dendritic field of SACs can be divided into proximal, intermediate and distal zones (Fig. 13). Their somata typically give rise to 4-6 primary dendrites, which may fork 2-3 branches in a short distance. The frequency of dividing becomes higher with

the dendrites traveling outward. Therefore, the outer the dendrites reach, the higher the branching density is. In addition, numerous varicosities are apparent at the distal dendrites (Fig. 13, 14), where the output synapses mainly located (Brandon, 1987; Famiglietti, 1991).

.

3.4 Dendritic contact patterns between a DSGC and a SAC

Co-fasciculation is defined as two or more dendrites exist side by side, and sometimes wind around. Theoretically, the more contacts between the dendritic segments, the more chance of synaptic sites may form. In order to examine whether the SAC dendrites of different portion have different contact levels with the DSGC, we injected a SAC immediately next to a DSGC (soma to soma distance less than 50 μm). In this way, the dendritic field of a DSGC could potentially be covered by the SAC dendrites radiated at all directions. Moreover, we injected the two cells with different dyes, thus they can be easily distinguished by colors (Fig. 15).

Twenty-five regions were demarcated after a low magnification scanning (Fig. 15A), and each region was individually scanned using higher magnification (except the empty ones). Because dendrites of DSGCs and SACs are not always located on the same focal plane, Z-sectioning was applied in all scanning to collect the stack of images.

The scanned regions were then divided into eight regions, which denote the directions sequentially for the following processing (Fig. 15B). We calculated the dendritic contact index (*DCI*) for each regions. Suppose that direction selectivity is generated by the asymmetric pattern of

contact between DSGCs and SACs, the maximum *DCI* value obtained should decline gradually in either clockwise or counterclockwise fashion, and reach the lowest *DCI* value in the opposite direction. The maximum *DCI* and the *DCI* of the two neighbor regions were summed and regarded as the preferred *DCI*, whereas the sum of the opposite three regions was the null *DCI*. The *DI* for the dendritic contacts can then be calculated.

Notably, the degree of dendritic contacts (or co-fasciculations) can only be faithfully revealed and calculated by high magnification (Fig. 16). No apparent difference of the contacts between each side of the dendrites of DSGCs and SACs can be seen. Quantified results of the dendritic contact patterns were included below.

3.5 Inhibitory synaptic patterns between a DSGC and a SAC

Having established that all sides of SAC dendrites non-selectively contact with a DSGC, we further examined the patterns of inhibitory synaptic inputs on a DSGC. Triple-labeling was originally conducted to perform this task. For some unknown reasons, the long-wavelength sensitive dyes (we tried Cy5 and Alexa fluor 635) were unfortunately bleached at an abnormal speed under the 633 helium-neon laser. Alternatively, both the DSGCs and its nearby SACs were injected using the same dye. Immnostaining was then processed to label the sites of the inhibitory synapses using an antibody against the alpha-1 subunit of $GABA_A$ receptors. Although co-localize between $GABA_A$ receptors and synaptophysins (or other synaptic structures) were not examined in

our experiment, past studies have built up a consensus that these $GABA_A$ puncta are functional (Greferath et al., 1995; Brandstatter et al., 1995; Fletcher et al., 1998; Euler and Wassle, 1998; Jeon et al., 2002). Colocalization of the injected cells (green) with $GABA_A$ receptors (red) is shown in Figure 17A-C, in which $GABA_A$ receptors were clustered in discrete puncta as previous reported (Koulen et al., 1996). The dendrites of DSGCs and SACs were separated carefully by hand, and $GABA_A$ puncta overlapped the dendrites were marked as well (Fig. 17D). The trace of complete dendrites and GABA inputs from the injected SAC are shown in Figure 18. The somata of the SACs were positioned in the center, and the cell pair together with the $GABA_A$ receptor puncta was divided into eight regions. The synaptic connection index (*SCI*) was computed for each regions. The maximum *SCI* and the *SCI* of the two neighbor regions were summed and regarded as the preferred *SCI*, whereas the sum of the opposite three regions was the null *SCI*. The *DI* for the synaptic connection can then be calculated. The inhibitory inputs on the DSGC dendrites can be found in all directions and appear to have a random distribution. No conspicuous pattern can be immediately recognized in the location of inputs on the DSGC dendrites. Figure 19 showed the *DI*s of the dendritic contact is 0.09 ± 0.04 (mean ± s.d., n=6), and the synaptic connection 0.08 ± 0.06 (n=3), whereas the *DI* of the spike response is 0.78 ± 0.16 (n=15). Although some cell pairs were inappropriate for quantification analysis (not all SAC dendrtites which projected in different directions were covered by the dendrites of DSGC, see supplementary figure 1), the regions where the DSGC and the SAC dendrites co-exists usually exhibit similar pattern.